The role of the stratospheric polar vortex for the austral jet response to greenhouse gas forcing

Geophysical Research Letters

RESEARCH LETTER
10.1029/2019GL082883

The Role of the Stratospheric Polar Vortex for the Austral Jet Response to Greenhouse Gas Forcing

Paulo Ceppi[1,2] **and Theodore G. Shepherd**[2]

[1]Grantham Institute for Climate Change and the Environment, Imperial College London, London, UK, [2]Department of Meteorology, University of Reading, Reading, UK

Abstract Future shifts of the austral midlatitude jet are subject to large uncertainties in climate model projections. Here we show that, in addition to other previously identified sources of intermodel uncertainty, changes in the timing of the stratospheric polar vortex breakdown modulate the austral jet response to greenhouse gas forcing during summertime (December–February). The relationship is such that a larger delay in vortex breakdown favors a more poleward jet shift, with an estimated 0.7–0.8° increase in jet shift per 10-day delay in vortex breakdown. The causality of the link between the timing of the vortex breakdown and the tropospheric jet response is demonstrated through climate modeling experiments with imposed changes in the seasonality of the stratospheric polar vortex. The vortex response is estimated to account for about 30% of the intermodel variance in the shift of the summertime austral jet and about 45% of the mean jet shift.

Key Points:
- Response of austral stratospheric polar vortex to CO_2 forcing is highly uncertain in CMIP5
- Larger delay in vortex breakdown favors larger poleward midlatitude jet shift in austral summer
- Vortex response accounts for about 30% of intermodel variance in austral summer jet shift and about 45% of the mean jet shift

Supporting Information:
- Supporting Information S1
- Figure S1
- Figure S2

Correspondence to:
P. Ceppi,
p.ceppi@imperial.ac.uk

Citation:
Ceppi, P., & Shepherd, T. G. (2019). The role of the stratospheric polar vortex for the austral jet response to greenhouse gas forcing. *Geophysical Research Letters*, *46*. https://doi.org/10.1029/2019GL082883

Received 18 MAR 2019
Accepted 3 MAY 2019
Accepted article online 9 MAY 2019

1. Introduction

In climate models, a common feature of the response to greenhouse gas forcing is a poleward shift of the midlatitude jets, particularly in the Southern Hemisphere (SH) (e.g., Barnes & Polvani, 2013; Kushner et al., 2001; Yin, 2005). Quantitative aspects of this response remain highly uncertain, however; as an example, the annual-mean austral jet shift in the Representative Concentration Pathway 8.5 (RCP8.5) scenario ranges from near 0° to about 4.5° poleward (Barnes & Polvani, 2013, their Figure 12). Such differences in jet response would be expected to have substantial impacts on regional climate, particularly in terms of the hydrological budget (Scheff & Frierson, 2012).

Previous literature has highlighted two main sources of structural uncertainty for the forced response of the zonal-mean austral jet. First, Kidston & Gerber (2010) proposed that the response is conditioned by the initial state, such that the poleward shift is larger in models where the jet is biased toward lower latitude. This relationship would be consistent with fluctuation-dissipation arguments, because lower-latitude jets are typically associated with longer time scales of annular mode variability (Barnes et al., 2010; Gerber & Vallis, 2007; Kidston & Gerber 2010; Ring & Plumb, 2008). These results have recently been called into question by Simpson and Polvani (2016), however, so the importance of the initial state for the forced response remains an open question.

A second source of uncertainty in the future austral jet response comes from changes in midlatitude baroclinicity (Harvey et al., 2014), themselves strongly influenced by the meridional sea surface temperature (SST) gradients (Ceppi & Shepherd, 2017; Ceppi et al., 2014; Chen et al., 2010). In general, an enhanced meridional temperature gradient (enhanced baroclinicity) favors a strengthening and poleward shift of the jet.

Here we highlight the stratosphere as an additional source of model uncertainty in the future austral jet response, relevant to the summer season (December–February, DJF). On interannual time scales, variability in the seasonal breakdown of the stratospheric polar vortex has been shown to modulate the transition from a poleward jet regime to a more equatorward one between late spring and early summer (Byrne et al., 2017; Byrne & Shepherd, 2018). In this regime-based perspective, the observed long-term poleward jet shift in response to ozone depletion during DJF can also be interpreted as a delayed equatorward transition of the jet, resulting from a delayed stratospheric polar vortex breakdown (VB) (Byrne et al., 2017; Sun et al., 2014). In this paper, we demonstrate that changes in the timing of the VB also affect the austral jet response

to greenhouse gas forcing and account for a substantial part of the intermodel uncertainty in the response during the summer season.

2. Data and Methods

Our analysis is based on output from the piControl and RCP8.5 experiments of the Coupled Model Intercomparison Project phase 5 (CMIP5). We define the RCP8.5 response as the difference between years 2080–2099 of RCP8.5 and a 20-year climatology from piControl. We use the piControl climate as a baseline rather than the present day in order to minimize the impact of stratospheric ozone on the results (see section 3 for further discussion), but note that our results are very similar if we use the 1950–1969 historical period as a baseline instead (not shown). We include the following 22 models in our analysis: ACCESS1-0, ACCESS1-3, BNU-ESM, CanESM2, CMCC-CESM, CMCC-CM, CMCC-CMS, CSIRO-Mk3-6-0, GFDL-ESM2G, GFDL-ESM2M, HadGEM2-CC, INMCM4, IPSL-CM5A-LR, IPSL-CM5A-MR, IPSL-CM5B-LR, MIROC-ESM, MIROC-ESM-CHEM, MIROC5, MPI-ESM-LR, MPI-ESM-MR, MRI-CGCM3, and NorESM1-M. The data analyzed include daily and monthly mean temperature, zonal wind, and meridional wind, all zonally averaged. To compare the model results with the real world, we also analyze the same variables in the European Centre for Medium Range Weather Forecasts Reanalysis 5 (ERA5) (Hersbach & Dee, 2016), using 39 austral summers between July 1979 and June 2018.

As in previous literature, we define the vortex strength using the daily mean zonal-mean zonal wind at 50 hPa and 60°S (Black & McDaniel, 2007; Byrne & Shepherd, 2018; Byrne et al., 2017; Sheshadri et al., 2015). The VB date is identified as the final time when the daily mean vortex strength drops below 15 m/s between spring and summer. While previous studies have used a threshold of 10 m/s to identify the VB date, in some CMIP5 models the vortex strength does not cross this threshold in the RCP8.5 climate, and therefore we use a slightly higher threshold. Results are very similar if we use an even higher threshold of 20 m/s, so the relationships are insensitive to the exact definition of VB. The tropospheric jet latitude is defined as the latitude of peak zonal-mean zonal wind at 850 hPa. The zonal wind fields are cubically interpolated to a 0.1° latitude grid prior to locating the jet position.

To test the causality of the relationships, we perform experiments with the Community Earth System Model (CESM) version 1.2.2, with the atmospheric component CAM4 and prescribed SSTs and sea ice. We use a high-top version of CAM4 with 46 vertical levels and a model top at 0.3 hPa. The code modifications are documented by Richter et al. (2015), but note that these authors used the newer CAM5 physics package. The horizontal resolution is 1.9° latitude × 2.5° longitude. The imposed monthly climatologies of SSTs and sea ice are taken from the RCP8.5 multimodel mean state. Atmospheric CO_2 concentration is set to 4 times its preindustrial value (4×284.7 ppm $= 1,138.8$ ppm), which approximates the late 21st century CO_2-equivalent forcing agent concentrations in RCP8.5, estimated at 1,084.4 ppm (based on data linked in footnote 6 of Meinshausen et al., 2011).

3. Changes in the Seasonality of the Austral Polar Vortex in RCP8.5

We first consider how the austral polar vortex climatology is predicted to change with global warming. Under RCP8.5 forcing, the vortex strengthens during much of the year and particularly in late austral spring (Figure 1), resulting in a delayed breakdown. The multimodel mean breakdown date shifts from 20 November to 8 December—an 18-day delay. This is a well-documented feature of the stratospheric polar vortex response to increased greenhouse gas concentrations in climate models (McLandress et al., 2010; Wilcox & Charlton-Perez, 2013). Note that although stratospheric ozone depletion also causes a delay in VB (McLandress et al., 2010; Sun et al., 2014; Wilcox & Charlton-Perez, 2013), the choice of periods for the calculation of the response (piControl and late 21st century) means that the ozone effect should be small, although not entirely negligible (e.g., Figure 13d of McLandress et al., 2010; Cionni et al., 2011 for the models using CMIP5 ozone forcing). The distinct peak in vortex strengthening in late November (Figure 1b) suggests that nonlinear wave-mean flow feedbacks reinforce the vortex response during the breakdown phase. From Figure 1b, it is also evident that the largest intermodel spread in vortex response occurs during the decay phase of the vortex; this is consistent with the seasonal cycle of interannual vortex variability (Baldwin et al., 2003, their Figure 1).

The VB date changes are shown in Figure 2 for individual climate models. While the VB is delayed in all models in RCP8.5 (Figure 2a), the intermodel spread in the response is very large, ranging from 5 to 33 days.

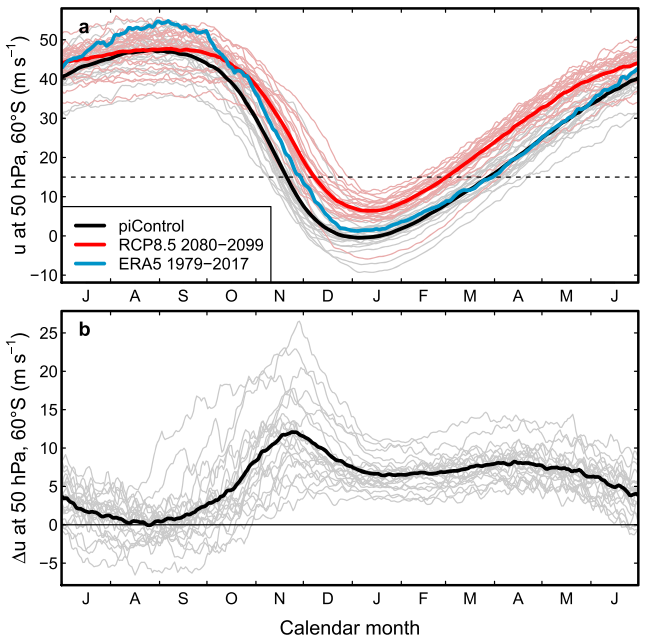

Figure 1. Daily climatology of the austral stratospheric polar vortex in CMIP5 and the ERA5 reanalysis, based on zonal-mean zonal wind at 50 hPa and 60°S. (a) Thin gray lines represent the piControl climatologies from individual climate models (multimodel mean in thick black), pale red lines denote the RCP8.5 climatologies (2080–2099; multimodel mean in thick red), and the thick blue line represents the ERA5 climatology. The horizontal dashed line denotes the 15-m/s threshold used to define the vortex breakdown date. (b) Thin gray lines show the vortex responses from individual climate models, calculated as RCP8.5 minus piControl (multimodel mean in thick black). CMIP5 = Coupled Model Intercomparison Project phase 5; RCP = Representative Concentration Pathway.

We estimate that the delay in VB is statistically significant at the 5% level in all models, based on a two-sided t test of the difference in means between the 20-year distributions of yearly VB dates in piControl and RCP8.5. In other words, the changes in VB date are incompatible with random natural variations in the polar vortex strength.

The changes in VB date are correlated with global warming across models, albeit weakly ($r = 0.26$), which is unsurprising given that global warming is a primary underlying driver of the vortex response. However, the stratospheric vortex also exhibits a weaker "direct" response to greenhouse gas forcing, akin to the direct jet stream response to CO_2 forcing discussed by Grise and Polvani (2014). We find that the vortex response to CO_2 quadrupling in isolation, taken as the difference between the amip4×CO_2 and amip experiments for a smaller set of seven models, involves a 6-day delay in breakdown date (not shown), confirming that global warming is not the sole driver of the response. We therefore assume that the vortex response ΔV can be approximated as $\Delta V \approx a\Delta T + b$; that is, ΔV includes a component proportional to global warming ΔT and another component independent of it. To remove the potentially confounding effects of different amounts of global warming in the different models, we regress out the global warming signal from the VB date changes (Figure 2b). By construction, the residuals have zero mean and zero linear correlation with global warming, but the responses still reflect differences in how each model responds to the same amount of global warming. Removing the global warming signal does not substantially reduce the spread in VB response ($\sigma = 7.9$ days in panel a vs. 7.6 days in panel b). Hereafter, the values in Figure 2b are referred to as the "vortex breakdown index" (VBI).

Interestingly, there is a suggestion that low-top models favor a larger delay in VB in RCP8.5, once the global warming effect is accounted for: The mean VBI is 6.4 days more positive for low-top models compared with high-top models. The difference between high- and low-top models is marginally statistically significant at the 5% level, based on a two-sided t test of the difference in means (p level = 0.047; 11 models in each group). While this is in contradiction with the results of Wilcox and Charlton-Perez (2013), there are several differences in methodology: (1) They use

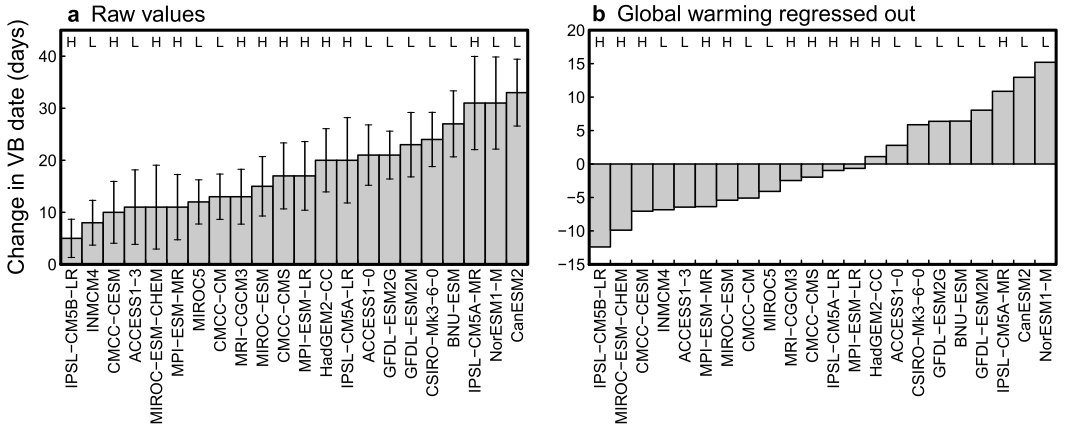

Figure 2. Changes in austral polar vortex breakdown date in RCP8.5 (2080–2099), relative to piControl. The letters H and L indicate whether a model is high or low top, where high top is defined as the model lid being above 1 hPa in altitude (Charlton-Perez et al., 2013). (a) All values are estimated to be significantly different from 0 at a p level of 5%, with the vertical bars denoting the 95% confidence intervals, based on a t test of the difference in means between the piControl and RCP8.5 climates. (b) The values are defined as the "vortex breakdown index" (VBI).
RCP = Representative Concentration Pathway; VB = vortex breakdown.

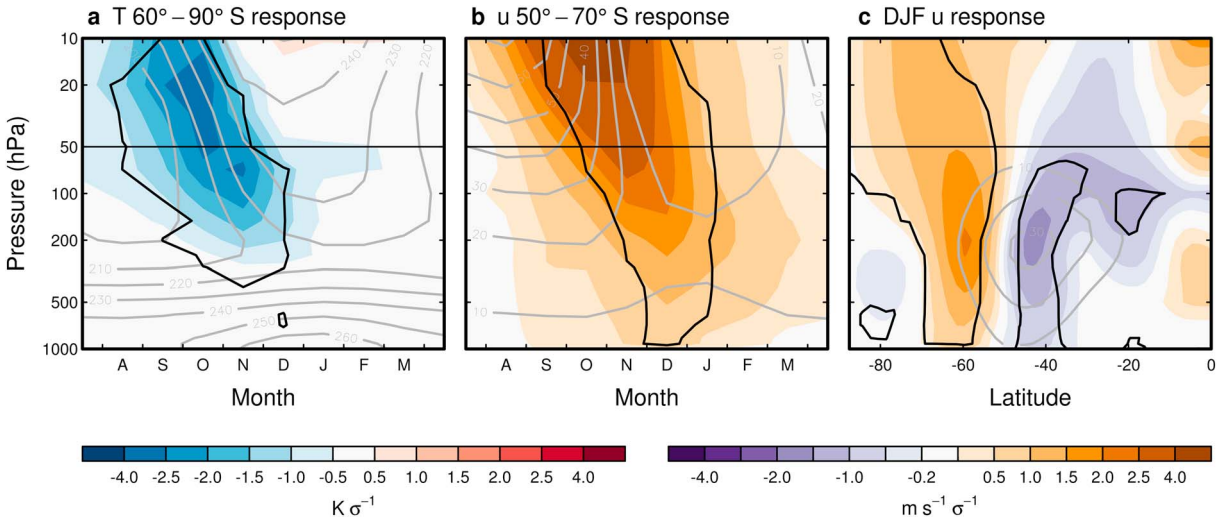

Figure 3. Time-pressure profiles of high-latitude zonal-mean temperature (a, 60°–90°S) and zonal wind (b, 50°–70°S) regressed onto the VBI. (c) The regression slope of zonal-mean zonal wind is shown as a function of latitude and pressure for DJF. In all panels the regression slopes are scaled for a 1 standard deviation VBI anomaly (σ = 7.6 days). The horizontal lines denote the 50-hPa level, used for the definition of the vortex breakdown. Black contours delineate regions where the regression slopes are statistically significant at a p level of 1%; gray contours indicate climatological values. Note that the global warming signal has been regressed out of the temperature and zonal wind responses prior to regressing onto the VBI. VBI = vortex breakdown index; DJF = December-January-February.

a temperature-based (rather than wind-based) measure of VB; (2) they use a smaller set of 14 models; and (3) they do not regress out the global warming signal. Given the small difference between high- and low-top models, we cannot reach a definitive conclusion regarding the effect of stratospheric resolution on the vortex response; further work would be needed to determine the robustness of this relationship but would be beyond the scope of this paper.

4. Downward Influence of the Austral Polar Vortex Response

There is robust evidence linking unforced variability in the stratospheric polar vortex to the state of the tropospheric midlatitude jet during summer in the SH, with a delayed VB corresponding to a poleward-shifted jet in December–February (DJF; Byrne et al., 2017; Thompson et al., 2005). Lagged regressions are suggestive of a downward causal path from the stratosphere to the troposphere, with the VB timing being influenced by the stratospheric state in preceding months; this provides a source of seasonal predictability of summertime annular mode anomalies from late winter onward (Byrne & Shepherd, 2018).

Here we hypothesize that the relationships between stratospheric polar vortex and tropospheric jet found in unforced variability also hold in the context of the forced response. If this is the case, then the uncertainty in vortex response identified in Figure 2 should be reflected in the SH jet response during DJF. To verify this, we show regressions of zonal-mean temperature and zonal wind responses in RCP8.5 onto the VBI (Figure 3). For consistency with the VBI definition, here and in subsequent figures the global warming signal has been regressed out of the RCP8.5 responses. Across CMIP5 models, a larger delay in the VB in RCP8.5 (i.e., positive VBI) is associated with stronger stratospheric cooling over the Antarctic cap from late winter to summer, with the cold anomaly peaking and propagating downward during spring. Importantly, a statistically significant poleward shift of the tropospheric jet is associated with the stratospheric anomalies during DJF (Figures 3b and 3c), supporting the hypothesis that changes in the timing of the SH VB exert an influence on the tropospheric jet response during austral summer. The tropospheric jet response becomes nonexistent from March onward (see also Figure 4 below).

We have also verified that the across-model relationships from Figure 3 are in good qualitative agreement with those found in unforced interannual variability in the ERA5 reanalysis, consistent with previous work (supporting information Figure S1; see also Byrne & Shepherd, 2018, Figure 5). The main differences relative to CMIP5 are in the lower stratosphere, where responses are larger during October–December in the reanalysis; moreover, the tropospheric jet anomalies tend to develop earlier in the reanalysis, being statistically significant in October. Furthermore, although the DJF zonal wind anomalies are slightly weaker in

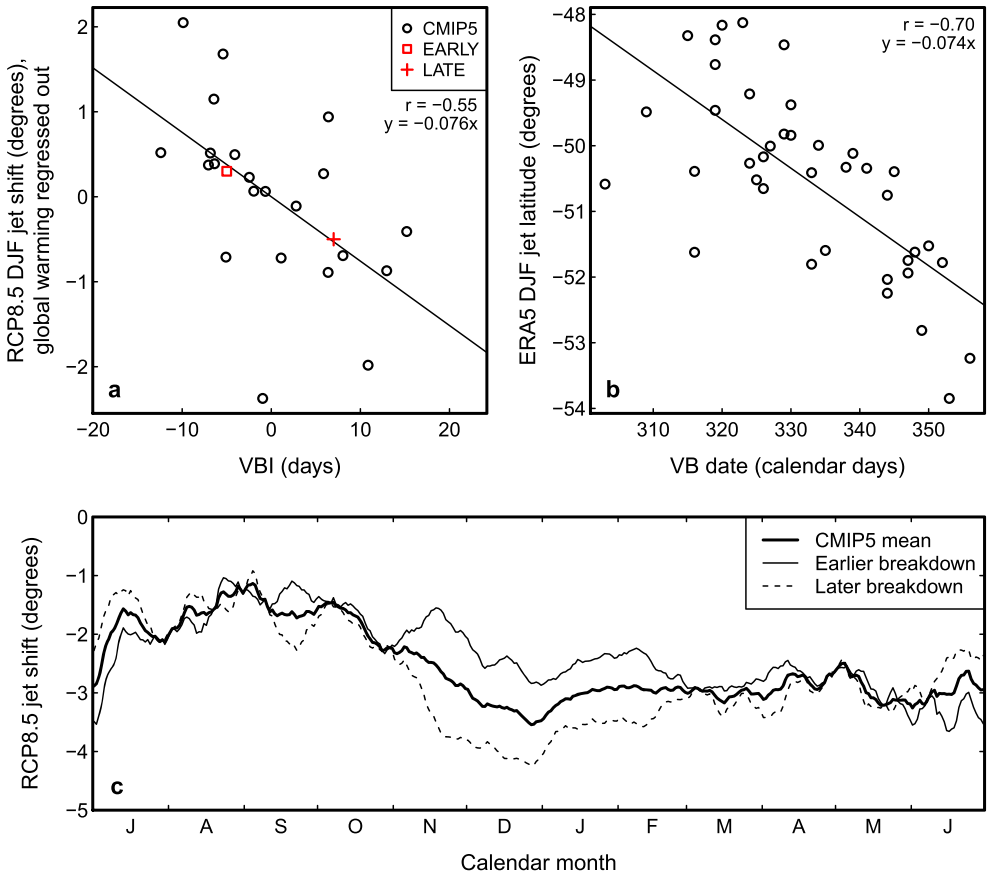

Figure 4. (a) DJF jet shift (global warming regressed out) versus VBI in RCP8.5, with each black circle representing a model. The red symbols correspond to the CAM4 nudging experiments EARLY and LATE (section 5), with the jet and VBI anomalies calculated relative to BASE. (b) DJF jet latitude versus vortex breakdown date in ERA5, with each circle representing a year. The lines represent least squares fits. (c) Annual cycle of the austral jet shift (before regressing out global-mean warming) based on 850-hPa daily zonal wind data, aggregated into 9-day running means. Shown are the multimodel mean (thick black curve) and the response to $\pm 1\sigma$ anomalies in VBI, calculated by regression analysis. The axes in (a) and (b) are scaled to have the same aspect ratio. DJF = December-January-February; VBI = vortex breakdown index; RCP = Representative Concentration Pathway.

the reanalysis, they project more strongly onto a shift since the node of the zonal wind dipole is closer to the climatological jet (compare Figures 3c and S1c).

The impact of the VB timing on the tropospheric jet in austral summer is summarized in Figure 4. In RCP8.5, the DJF jet shift (in degrees, positive northward) is negatively correlated with the VBI, such that with a larger delay in VB comes a more poleward jet shift (Figure 4a). Note that the mean jet shift in Figure 4a is 0 because global warming has been regressed out. The jet actually shifts poleward in all models, with a mean shift of 3.1°; the VB simply modulates the magnitude of that shift. The across-model relationship in the responses is again consistent with interannual variability in ERA5 (Figure 4b): years with a delayed VB feature a poleward jet anomaly in DJF. (Note that although the ERA5 results include a positive ozone-induced trend in VB dates, the correlation and slope remain essentially unchanged if the indices are detrended; not shown.) The slopes of the relationships indicate a 0.7–0.8° poleward shift of the jet per 10-day delay in VB. The similarity of the slopes between Figures 4a and 4b suggests that on average, models and observations are in qualitative agreement on the impact of the VB timing on the SH jet position in austral summer. Note, however, that the VBI statistically accounts for only about 30% of the CMIP5 intermodel variance in DJF jet shift, indicating that other factors must contribute to the uncertainty (see section 6 for further discussion).

The full seasonal cycle of the austral jet shift, and its dependence on the vortex response, are shown in Figure 4c. Consistent with Figure 3, the change in VB date affects the jet response between November and February. Using the slope of the relationship in Figure 4a, we estimate that the mean delay in VB date of 18

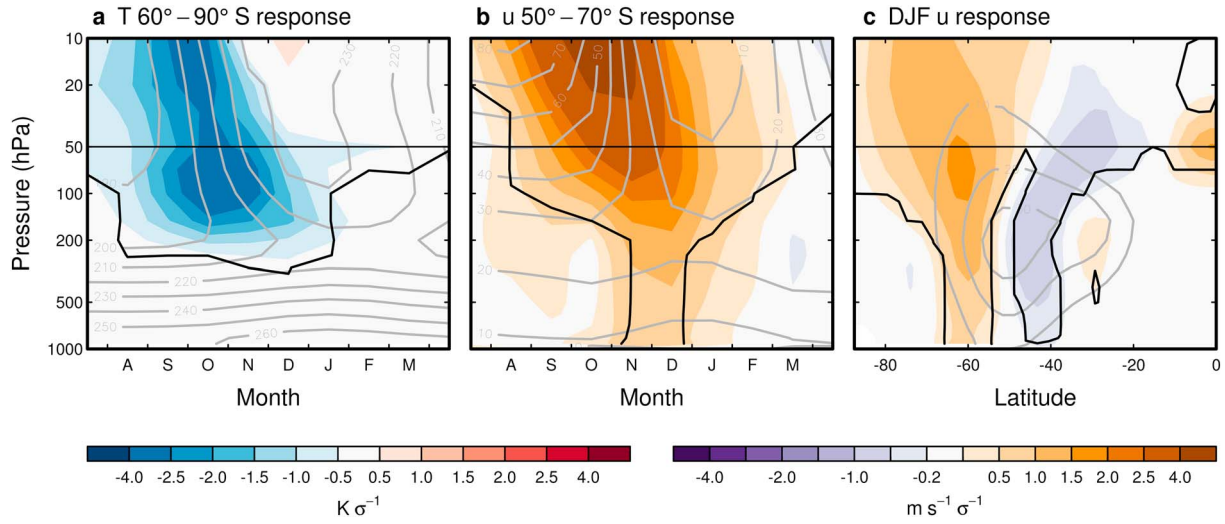

Figure 5. As in Figure 3, but showing monthly responses in the CAM4 nudging experiments. The responses are scaled to correspond to a 1σ VBI change in CMIP5 (7.6 days).

days enhances the DJF poleward jet shift by about 1.4°—close to half (45%) of the multimodel mean shift of 3.1°.

5. Modeling Experiments

In the context of interannual variability, the timing of the relationship between VB and austral jet position in DJF suggests a downward causal link, because the stratospheric anomalies precede the tropospheric wind anomalies (Byrne & Shepherd, 2018; Byrne et al., 2017). When considering intermodel differences in the response to greenhouse gas forcing, however, we cannot rule out that the relationship between VBI and DJF jet shift results from a common driving factor, rather than being causal. As an example, one could hypothesize that intermodel differences in the formulation of the dynamical core affect both the vortex response and the austral jet shift. Therefore, to confirm the causal link between polar vortex and tropospheric jet responses, we perform climate model experiments in which the stratosphere is nudged toward prescribed climatologies (see section 2 for details on the model).

We first run a 100-year baseline experiment with RCP8.5 conditions and no nudging, from which we derive a 6-hourly climatology of instantaneous values, which serves as the basis for all nudging experiments. The nudging procedure follows Simpson et al. (2018), and the details are described in the supporting information (Text S1), but we summarize the key features of the experiments here. Full nudging is applied only for altitudes above 28 hPa, and the nudging tendencies are linearly tapered to 0 from 28 to 64 hPa. The variables nudged are temperature, zonal wind, and meridional wind. We perform three nudging simulations, all of which are run for 100 years. In the first (BASE), we nudge the model toward its own 6-hourly stratospheric climatology, which allows us to verify that nudging has only minimal impact on the model's climate (not shown). The remaining two simulations (EARLY and LATE) have stratospheric anomalies corresponding to $\pm 1\sigma$ in VBI added onto the BASE nudging climatology, where $\sigma = 7.6$ days. These anomalies are based on across-model regressions onto the VBI as shown in Figure 3 but are extended up to the model top at 0.3 hPa following the procedure described in the supporting information (Text S1 and Figure S2).

Figure 5 shows the monthly responses to the imposed stratospheric anomalies, based on the difference LATE minus EARLY, scaled so as to be consistent with a 1σ increase in the VBI—a 7.6-day delay in VB date. (Although the model is forced with $\pm 1\sigma$ VBI anomalies, the resulting VB responses are slightly weaker: −5 days in EARLY and +7 days in LATE. This is likely because we have imposed the anomalies in the form of nudging tendencies, rather than imposing the anomalies themselves.) The model successfully reproduces the main features of the temperature and zonal wind evolution associated with a delayed VB, including the downward propagating polar temperature anomalies during spring, and the tropospheric jet response from late austral spring to late summer (Figure 5). The resulting DJF jet latitude anomalies are also in very good agreement with the CMIP5 relationship (red symbols in Figure 4a). Note that the individual responses in

EARLY and LATE are qualitatively similar, as evidenced by the fact that the jet-VBI relationship is similar in both experiments (Figure 4a), suggesting the response is approximately linear.

6. Summary and Discussion

We have demonstrated that in CMIP5 models forced with the RCP8.5 emissions scenario, the response of the Southern Hemispheric stratospheric polar vortex (relative to piControl) affects the austral jet response during summertime (DJF): The larger the delay in VB, the more the jet tends to shift poleward. This effect is consistent with the downward propagation of stratospheric vortex anomalies into the troposphere on interannual time scales as found in reanalysis data (Baldwin & Dunkerton, 2001; Black & McDaniel, 2007; Byrne et al., 2017; Byrne & Shepherd, 2018; Thompson et al., 2005). We estimate that with a 10-day delay in VB date comes a poleward jet shift of 0.7–0.8° in DJF. For the multimodel mean response, this implies that the mean delay in VB (18 days) accounts for about 45% of the mean DJF poleward jet shift of 3.1°.

The change in VB date statistically accounts for only 30% of the intermodel variance in DJF jet shift, however, reflecting the fact that the stratospheric polar vortex is not the sole factor contributing to the uncertainty in the jet response to greenhouse gas forcing. Among other important factors noted in previous research are the basic state, where a more equatorward jet favors a larger poleward shift (Kidston & Gerber 2010, but note that this relationship is weak in DJF, as shown by Simpson & Polvani, 2016), and changes in the meridional temperature gradient and baroclinicity around the midlatitudes (Harvey et al., 2014), possibly influenced by cloud-induced radiative changes (Ceppi & Hartmann, 2016; Ceppi & Shepherd, 2017; Voigt & Shaw, 2015). The relative contributions of these various driving factors to the intermodel uncertainty could be quantified using a statistical approach (Harvey et al., 2014; Manzini et al., 2014; Zappa & Shepherd, 2017) or model experiments (Ceppi & Shepherd, 2017; Harvey et al., 2015).

Given the large uncertainty in the austral stratospheric vortex response to forcing and the associated tropospheric impacts, there is a need for constraints on future vortex changes based on theory and observations. We find that in CMIP5 models, the VB change (Figure 2a) is relatively weakly correlated with the climatological VB date in piControl ($r = -0.41$; $r = -0.38$ if global warming is regressed out), suggesting that while the initial state affects the vortex response, other factors must also be at play. Understanding and quantifying the contributions to the vortex response will be the subject of future work.

Acknowledgments
P. C. was supported by an Imperial College Research Fellowship. T. G. S. was supported by ERC Advanced Grant "ACRCC" (grant 339390). We thank two anonymous reviewers for comments that helped improve the manuscript. We are very grateful to Yaga Richter and Isla Simpson for sharing the model code and for technical support with the simulations. We acknowledge the World Climate Research Programme's Working Group on Coupled Modelling, which is responsible for CMIP, and thank the climate modeling groups (listed in section 2 of this paper) for producing and making available their model output. For CMIP the U.S. Department of Energy's Program for Climate Model Diagnosis and Intercomparison provides coordinating support and led the development of software infrastructure in partnership with the Global Organisation for Earth System Science Portals. This work used the ARCHER UK National Supercomputing Service (http://www.archer.ac.uk). The CAM4 experiment output can be downloaded from https://doi.org/10.6084/m9.figshare.7859534.

References

Baldwin, M. P., & Dunkerton, T. J. (2001). Stratospheric harbingers of anomalous weather regimes. *Science*, *294*(5542), 581–4. https://doi.org/10.1126/science.1063315

Baldwin, M. P., Stephenson, D. B., Thompson, D. W. J., Dunkerton, T. J., Charlton, A. J., & O'Neill, A. (2003). Stratospheric memory and skill of extended-range weather forecasts. *Science*, *301*(5633), 636–40. https://doi.org/10.1126/science.1087143

Barnes, E. A., Hartmann, D. L., Frierson, D. M. W., & Kidston, J. (2010). Effect of latitude on the persistence of eddy-driven jets. *Geophysical Research Letters*, *37*, L11804. https://doi.org/10.1029/2010GL043199

Barnes, E. A., & Polvani, L. (2013). Response of the midlatitude jets and of their variability to increased greenhouse gases in the CMIP5 models. *Journal of Climate*, *26*(18), 7117–7135. https://doi.org/10.1175/JCLI-D-12-00536.1

Black, R. X., & McDaniel, B. A. (2007). Interannual variability in the Southern Hemisphere circulation organized by stratospheric final warming events. *Journal of the Atmospheric Sciences*, *64*(8), 2968–2974. https://doi.org/10.1175/JAS3979.1

Byrne, N. J., & Shepherd, T. G. (2018). Seasonal persistence of circulation anomalies in the Southern Hemisphere stratosphere and its implications for the troposphere. *Journal of Climate*, *31*(9), 3467–3483. https://doi.org/10.1175/JCLI-D-17-0557.1

Byrne, N. J., Shepherd, T. G., Woollings, T., & Plumb, R. A. (2017). Nonstationarity in Southern Hemisphere climate variability associated with the seasonal breakdown of the stratospheric polar vortex. *Journal of Climate*, *30*(18), 7125–7139. https://doi.org/10.1175/JCLI-D-17-0097.1

Ceppi, P., & Hartmann, D. L. (2016). Clouds and the atmospheric circulation response to warming. *Journal of Climate*, *29*(2), 783–799. https://doi.org/10.1175/JCLI-D-15-0394.1

Ceppi, P., & Shepherd, T. G. (2017). Contributions of climate feedbacks to changes in atmospheric circulation. *Journal of Climate*, *30*, 9097–9118. https://doi.org/10.1175/JCLI-D-17-0189.1

Ceppi, P., Zelinka, M. D., & Hartmann, D. L. (2014). The response of the Southern Hemispheric eddy-driven jet to future changes in shortwave radiation in CMIP5. *Geophysical Research Letters*, *41*, 3244–3250. https://doi.org/10.1002/2014GL060043

Charlton-Perez, A. J., Baldwin, M. P., Birner, T., Black, R. X., Butler, A. H., Calvo, N., et al. (2013). On the lack of stratospheric dynamical variability in low-top versions of the CMIP5 models. *Journal of Geophysical Research: Atmospheres*, *118*, 2494–2505. https://doi.org/10.1002/jgrd.50125

Chen, G., Plumb, R. A., & Lu, J. (2010). Sensitivities of zonal mean atmospheric circulation to SST warming in an aqua-planet model. *Geophysical Research Letters*, *37*, L12701. https://doi.org/10.1029/2010GL043473/abstract

Cionni, I., Eyring, V., Lamarque, J. F., Randel, W. J., Stevenson, D. S., Wu, F., et al. (2011). Ozone database in support of CMIP5 simulations: Results and corresponding radiative forcing. *Atmospheric Chemistry and Physics*, *11*(21), 11,267–11,292. https://doi.org/10.5194/acp-11-11267-2011

Gerber, E. P., & Vallis, G. K. (2007). Eddy-zonal flow interactions and the persistence of the zonal index. *Journal of the Atmospheric Sciences*, *64*(9), 3296–3311. https://doi.org/10.1175/JAS4006.1

Grise, K. M., & Polvani, L. M. (2014). The response of midlatitude jets to increased CO_2: Distinguishing the roles of sea surface temperature and direct radiative forcing. *Geophysical Research Letters*, *41*, 6863–6871. https://doi.org/10.1002/2014GL061638

Harvey, B. J., Shaffrey, L. C., & Woollings, T. J. (2014). Equator-to-pole temperature differences and the extra-tropical storm track responses of the CMIP5 climate models. *Climate Dynamics*, *43*(5-6), 1171–1182. https://doi.org/10.1007/s00382-013-1883-9

Harvey, B. J., Shaffrey, L. C., & Woollings, T. J. (2015). Deconstructing the climate change response of the Northern Hemisphere wintertime storm tracks. *Climate Dynamics*, *45*(9-10), 2847–2860. https://doi.org/10.1007/s00382-015-2510-8

Hersbach, H., & Dee, D. P. (2016). ERA5 reanalysis is in production. *ECMWF Newsletter*, *147*(7), 5–6.

Kidston, J., & Gerber, E. P. (2010). Intermodel variability of the poleward shift of the austral jet stream in the CMIP3 integrations linked to biases in 20th century climatology. *Geophysical Research Letters*, *37*, L09708. https://doi.org/10.1029/2010GL042873

Kushner, P. J., Held, I. M., & Delworth, T. L. (2001). Southern Hemisphere atmospheric circulation response to global warming. *Journal of Climate*, *14*(10), 2238–2249. https://doi.org/10.1175/1520-0442(2001)014h0001:SHACRTi2.0.CO;2

Manzini, E., Karpechko, A. Y., Anstey, J., Baldwin, M. P., Black, R. X., Cagnazzo, C., et al. (2014). Northern winter climate change: Assessment of uncertainty in CMIP5 projections related to stratosphere-troposphere coupling. *Journal of Geophysical Research: Atmospheres*, *119*, 7979–7998. https://doi.org/10.1002/2013JD021403

McLandress, C., Jonsson, A. I., Plummer, D. A., Reader, M. C., Scinocca, J. F., & Shepherd, T. G. (2010). Separating the dynamical effects of climate change and ozone depletion. Part I: Southern Hemisphere stratosphere. *Journal of Climate*, *23*(18), 5002–5020. https://doi.org/10.1175/2010JCLI3586.1

Meinshausen, M., Smith, S. J., Calvin, K., Daniel, J. S., Kainuma, M. L. T., Lamarque, J.-F., et al. (2011). The RCP greenhouse gas concentrations and their extensions from 1765 to 2300. *Climatic Change*, *109*(1-2), 213–241. https://doi.org/10.1007/s10584-011-0156-z

Richter, J. H., Deser, C., & Sun, L. (2015). Effects of stratospheric variability on El Niño teleconnections. *Environmental Research Letters*, *10*(12), 124021. https://doi.org/10.1088/1748-9326/10/12/124021

Ring, M. J., & Plumb, R. A. (2008). The response of a simplified GCM to axisymmetric forcings: Applicability of the fluctuation dissipation theorem. *Journal of the Atmospheric Sciences*, *65*(12), 3880–3898. https://doi.org/10.1175/2008JAS2773.1

Scheff, J., & Frierson, D. (2012). 21st-century multi-model subtropical precipitation declines are mostly mid-latitude shifts. *Journal of Climate*, *25*, 4330–4347. https://doi.org/10.1175/JCLI-D-11-00393.1

Sheshadri, A., Plumb, R. A., & Gerber, E. P. (2015). Seasonal variability of the polar stratospheric vortex in an idealized AGCM with varying tropospheric wave forcing. *Journal of the Atmospheric Sciences*, *72*(6), 2248–2266. https://doi.org/10.1175/JAS-D-14-0191.1

Simpson, I. R., Hitchcock, P., Seager, R., Wu, Y., & Callaghan, P. (2018). The downward influence of uncertainty in the Northern Hemisphere stratospheric polar vortex response to climate change. *Journal of Climate*, *31*(16), 6371–6391. https://doi.org/10.1175/JCLI-D-18-0041.1

Simpson, I. R., & Polvani, L. M. (2016). Revisiting the relationship between jet position, forced response and annular mode variability in the southern mid-latitudes. *Geophysical Research Letters*, *43*, 1–8. https://doi.org/10.1002/2016GL067989

Sun, L., Chen, G., & Robinson, W. A. (2014). The role of stratospheric polar vortex breakdown in Southern Hemisphere climate trends. *Journal of the Atmospheric Sciences*, *71*(7), 2335–2353. https://doi.org/10.1175/JAS-D-13-0290.1

Thompson, D. W. J., Baldwin, M. P., & Solomon, S. (2005). Stratosphere-troposphere coupling in the Southern Hemisphere. *Journal of the Atmospheric Sciences*, *62*(3), 708–715. https://doi.org/10.1175/JAS-3321.1

Voigt, A., & Shaw, T. A. (2015). Circulation response to warming shaped by radiative changes of clouds and water vapour. *Nature Geoscience*, *8*(2), 102–106. https://doi.org/10.1038/ngeo2345

Wilcox, L. J., & Charlton-Perez, A. J. (2013). Final warming of the Southern Hemisphere polar vortex in high- and low-top CMIP5 models. *Journal of Geophysical Research: Atmospheres*, *118*, 2535–2546. https://doi.org/10.1002/jgrd.50254

Yin, J. H. (2005). A consistent poleward shift of the storm tracks in simulations of 21st century climate. *Geophysical Research Letters*, *32*, L18701. https://doi.org/10.1029/2005GL023684/abstract

Zappa, G., & Shepherd, T. G. (2017). Storylines of atmospheric circulation change for European regional climate impact assessment. *Journal of Climate*, *30*(16), 6561–6577. https://doi.org/10.1175/JCLI-D-16-0807.1